SCIENTIFIC REPORTS

OPEN

SUBJECT AREAS:
NON-SMALL-CELL LUNG CANCER
LYMPHOCYTE ACTIVATION

Received
11 August 2014

Accepted
12 November 2014

Published
10 December 2014

Correspondence and requests for materials should be addressed to S.F. (Susetta.Finotto@uk-erlangen.de)

* These authors contributed equally to this work.

Increased expression of the Th17-IL-6R/pSTAT3/BATF/RorγT-axis in the tumoural region of adenocarcinoma as compared to squamous cell carcinoma of the lung

Ljubov Balabko[1]*, Katerina Andreev[1]*, Nadine Burmann[1]*, Melanie Schubert[1], Martina Mathews[1], Denis I. Trufa[2], Sarah Reppert[1], Tilmann Rau[3], Martin Schicht[4], Horia Sirbu[2], Arndt Hartmann[3] & Susetta Finotto[1]

[1]Department of Molecular Pneumology, Friedrich-Alexander-University Erlangen-Nürnberg (FAU), Erlangen, Germany, [2]Department of Thoracic Surgery, Friedrich-Alexander-University Erlangen-Nürnberg (FAU), Erlangen, Germany, [3]Institute of Pathology, Friedrich-Alexander-University Erlangen-Nürnberg (FAU), Erlangen, Germany, [4]Department of Anatomy II, Friedrich-Alexander-University Erlangen-Nürnberg (FAU), Erlangen, Germany.

Here we describe increased expression of *IL6R* in the tumoural region of lung tissue from patients affected by lung adenocarcinoma as compared to squamous cell lung carcinoma. Moreover, here we found increased *IL6R* in the tumour free part of the lung. By using a murine model of lung adenocarcinoma, we discovered that few lung tumour cells expressed IL-6R and CD4+CD25+Foxp-3+ T regulatory cells down-regulated IL-6R in the tumour bearing lungs. Downstream of IL-6R, the Th17 lineage-specification factors: Signal transducer and activator of transcription 3 (STAT3), Basic leucine zipper transcription factor, BATF and a protein encoded by the RORC in human (RAR-related orphan receptor C) (RORγT), were also found induced in the tumoural region of lung tissue from patients affected by lung adenocarcinoma as compared to those carrying squamous cell carcinoma. Moreover, pSTAT3 protein was found phosphorylated and auto-phosphorylated in the tumoural region of patients with adeno cell carcinoma of the lung as compared to the tumoural region of patients with squamous cell carcinoma of the lung. Intranasal application of anti-IL-6R antibodies in a murine model of lung adenocarcinoma, induced T regulatory cell markers such as *Foxp3*, *Ctla4*, *Icos*, *Il10*, *Il21*, *Folr4* and *Lag3* and inhibited *Rorc* in lung adenocarcinoma.

Lung cancer is the leading cause of cancer deaths world-wide and lung adenocarcinoma is one of the predominant histological subtypes of lung cancer (40%) followed by squamous (30%) and large cell lung carcinoma among non-small-cell lung cancers (NSCLC), which represent 85% of all lung tumours[1]. The development of these tumours is not only initiated by smoking but can be also attributed to genetic spontaneous mutations[2]. Epithelial cells are initially transformed into lung carcinomas[3]. Most of lung cancer cell lines including those with Epidermal-growth factor receptor (EGFR) mutations harbour auto-phosphorylated STAT3 that cannot be inhibited by EGFR inhibitors. By contrast, inhibitors of JAK1 and IL-6 resulted in reduced lung tumour cell growth and inhibition of STAT3 phosphorylation[4].We have previously demonstrated that delivery of anti-IL-17A antibody could successfully reduce lung tumour load, resulting in up-regulation of the Th1/Tc1 cytotoxicity and reduction of immunosuppressive regulatory CD4+CD25+FOXP3+ T cells in a murine model of lung adenocarcinoma. These data indicate Th17 cells as a potential target for immunotherapy against lung adenocarcinoma[5].

IL-6 along with TGF-β, which is present in the tumour microenvironment, induces Th17 cells and IL-6$^{-/-}$ mice have reduced Th17 cell development[6].

After binding of IL-6 to its receptor (IL-6R), JAK1-Tyk-2 and STAT3 are activated, resulting in STAT3 phosphorylation-dimerization and translocation into the nucleus[7]. Consistent with a role of STAT3 in Th17 differentiation, STAT3-CD4- conditional deficient mice have reduced Th17 cells[8].

Finally, downstream of IL-6, STAT3, RORγT and BATF cooperate to induce IL-17A gene[9,10].

BATF is a newly described transcription factor crucial for the differentiation of IL-17A-secreting Th17 cells, which play a pathogenic role in lung adenocarcinoma development[5,7,11,12]. BATF is a new member of the ATF/CREB family of transcription factors that has been isolated from a cDNA library prepared from Epstein-Barr virus stimulated human B cells and that showed the strongest hybridization in lung and Raji Burkitt's lymphoma by Northern blot analysis. More than ninety percent of mice overexpressing human BATF in T cells by 1 year of age develop a lymphoproliferative disorder (LPD). Moreover, the human oncoprotein JunB is a specific binding partner of BATF[13].

We thus thought to clarify the role of IL-6 signaling on the Th17 pathway in lung cancer tumour-infiltrating lymphocytes (TIL) as well as in lung cancer cells in different subtypes of NSCLC, considering that STAT3 is also an oncogene whose activation has been linked to EGFR mutation, which are present in lung cancer[12].

Results

Analysis of the cohorts of patients with adenocarcinoma versus squamous carcinoma of the lung. The clinical characteristics of the patients analysed in this study are reported in Table I.

In this study, we isolated mRNA and proteins from the tumoural and control regions (tumour-free) of two cohorts of patients with squamous cell carcinoma (SCC) and adenocarcinoma (ADC) of the lung. Moreover, we performed cryosections of the tumoural and control lung regions from OCT frozen lung tissues. The control region was taken at least 5 cm far away from the outer edge of the tumoural region (Fig. S1).

IL-6R is increased in the control region of NSCLC and in the tumoural region of ADC as compared to the tumoural region of SCC. IL-6 signals after its binding to the IL-6 receptor (IL-6R) alpha chain. We thus analysed the expression of the *IL-6RA* mRNA in NSCLC. Here we found a significant up-regulation of *IL-6RA* mRNA in the control region of both adeno- and squamous cell carcinoma as compared to the respective tumoural region (Fig. 1a). Moreover, *IL-6RA* mRNA was found significantly induced in the tumoural region of ADC as compared to the tumoural region of SCC (Fig. 1a, right handside). Altogether, these data indicate that *IL-6RA* mRNA expression is induced in the tumour region of adenocarcinoma bearing lungs as compared to the tumoural region of SCC. Moreover, there seems to be in both histological types of cancer a down-regulation of IL-6R expressing cells in the tumoural region. This could also be confirmed by immunohistochemical staining of IL-6R on tissue sections from the control and the tumoural lung region of patients with squamous as well as adenocarcinoma (Fig. 1 c).

The tumour cells used to induce experimental lung adenocarcinoma do not express IL-6R. To start to investigate whether the down-regulation of IL-6R in the tumoural region was due to the lack of IL-6R in the tumour cells, we analysed IL-6R expression by flow cytometry in the murine tumour cell line LL/2-luc-M38, used to induce experimental lung adenocarcinoma (Fig 1b). As shown, the lung adenocarcinoma cell line did not express IL-6R as this staining was comparable to the negative control. These findings probably explain why *IL-6RA* is down-regulated in the tumoural region of the patients with NSCLC.

CD4+CD25+FOXP-3+ T regulatory cells in lung adenocarcinoma tumour bearing mice down-regulated IL-6R. We have previously demonstrated that IL-6R alpha chain is expressed on lung CD4+CD25+Foxp-3+ T regulatory cells and that blockade of IL-6R induces T regulatory cells[14]. Lung adenocarcinoma is characterized by increased FOXP-3, which is a transcription factor signature of T regulatory cells[5]. We thus looked in the murine model of lung adenocarcinoma at the distribution of IL-6R expression in CD4+ T effector and CD4+CD25+FOXP-3+ T regulatory cells. Here we found that the number of lung CD4+ T cells bearing the IL-6R did not change in the lungs of naïve mice as compared to those present in the lungs of mice bearing tumour (Fig. 2a). However, we found a significant down-regulation of IL-6R alpha expression on the CD4+CD25+FOXP-3+ T regulatory cells present in mice bearing tumour (Fig. 2b).

In conclusion, in mice bearing tumour both tumour cells and CD4+CD25+FOXP-3+ T regulatory cells down-regulate IL-6R.

Increased *BATF* gene expression in the tumoural region of patients with lung adenocarcinoma (ADC) as compared to squamous cell carcinoma (SCC). Downstream of IL-6R, BATF is activated[13]. We thus asked if BATF was also up-regulated in the adenocarcinoma. Here we found that *BATF* mRNA is significantly increased in the tumour region of patients affected by lung adenocarcinoma as compared to the level measured in tissue derived from the tumour region of patients affected by lung squamous cell carcinoma (Fig. 3a, right hand side), suggesting a local induction of Th17 responses specific for adenocarcinoma but not for squamous cell carcinoma in the tumoural region. Consistently, by immunohistochemistry, BATF protein was found significantly up-regulated in the tumour region of patients with adenocarcinoma as compared to the tumoural region of patients with squamous cell carcinoma (Fig. 3b and 3c, respectively). Interestingly, in the control region of the lung of patients with squamous cell carcinoma, BATF was significantly induced as compared to the tumoural region (Fig. 3a). No difference in the distribution of *BATF* mRNA was observed in adenocarcinoma patients between control and tumoural regions.

Finally, in a murine model of lung adenocarcinoma, we found that CD4+ T cells, isolated from the lungs of mice bearing lung cancer cells, expressed significantly elevated levels of *Batf* mRNA as compared to those isolated from the lungs of naïve mice (Fig. 3 d–e).

Increased phospho- and autophosphorylation of STAT3 in the tumoral region of lung tissue from patients affected by adenocarcinoma as compared to those with squamous cell carcinoma. Downstream of IL-6R, upon IL-6 binding to IL-6R alpha, JAKs are activated. Subsequently, the gp130 tails are phosphorylated, which mediates the recruitment of the STAT3 proteins. Dimerization of activated (phosphorylated) STAT3 is followed by nuclear entry. Within the nucleus, STAT3 can enhance the transcription of many genes, including those that encode acute-phase proteins[9]. Consistent with the up-regulation of *Batf*, we found an up-regulation of *Stat3* mRNA in the lungs of tumour bearing mice as compared to tumour free animals (Fig. 3f).

Similarly, we next found an up-regulation of *STAT3* mRNA in the tumoural region of lung adenocarcinoma as compared to the tumoural region of squamous carcinoma (Fig. 4a). Moreover, we found a down-regulation of *STAT3* mRNA in the tumoural region of squamous cell carcinomas compared to the respective control region. By contrast, *STAT3* mRNA was comparable in the control and tumoural region of the adenocarcinoma groups (Fig. 4a). WE next thought to investigate if there was an auto activation of STAT3 ongoing in the tumoural region of adenocarcinoma. To do so, we analysed proteins isolated from the different regions of NSCLC by western blot analysis. We then analysed the phosphorylation state of STAT3 protein in these tissues and found significantly increased phosphorylation of STAT3 at both tyrosine (pY-STAT3: phosphotyrosine) (Fig. 4b and e–f) and serine (pS-STAT3: phosphoserine) (Fig. 4c and e–f) residues, in the tumoral region of adenocarcinoma as compared to squamous carcinoma (Fig 4. and Supplementary Fig. 2).

In conclusion, STAT3 was found increased and phosphorylated in the tumoural region of adenocarcinoma whereas there was no phosphorylation in the tumoural area of squamous carcinoma (Fig. 4e versus f, respectively). These findings are consistent with

Table I | Clinical data of the patients analysed in this study

Patient Number	Sample-ID	Histological Classification	Grading	T	N	M	Gender	Age
1	P2	ADC	G3	3	0	0	Male	69
2	P4	ADC	G3	3	0	0	Male	63
3	P5	ADC	G3	2b	0	0	Male	71
4	P6	ADC	G3	2	2	#	Female	64
5	P7	ADC	G3	3	0	0	Male	68
6	P12	ADC	G3	2b	1	0	Male	70
7	P14	ADC	G1	4	0	1	Male	75
8	P20	ADC	G3	2	0	0	Male	64
9	P22	ADC	G3	2a	1	0	Male	69
10	P26	ADC	G3	3	0	0	Male	48
11	P27	ADC	G2	1	0	0	Female	63
12	P28	ADC	G2	1b	0	0	Female	38
13	P31	ADC	G2	1b	2	0	Female	70
14	P33	ADC	G2	2b	2	0	Male	57
15	P37	ADC	G3	2a	0	0	Male	51
16	P38	ADC	G3	1a	0	0	Female	37
17	3-MP-IL35	ADC	G3	2a	0	0	Male	79
18	9-MP-IL35	ADC	G2	1b	2	0	Female	84
19	15-MP-IL35	ADC	G3	1b	0	0	Male	63
20	16-MP-IL35	ADC	G3	3	0	0	Female	70
21	17-MP-IL35	ADC	G2	2	0	0	Male	74
22	19-MP-IL35	ADC	#	2b	0	0	Female	55
23	22-MP-IL35	ADC	G3	2b	1	0	Male	68
24	23-MP-IL35	ADC	G2	2a	0	0	Male	73
25	26-MP-IL35	ADC	G3	1a	0	1	Female	52
26	27-MP-IL35	ADC	G3	1a	0	0	Female	70
27	28-MP-IL35	ADC	G3	1a	0	0	Male	76
28	32-MP-IL35	ADC	G3	2a	2	0	Female	60
29	34-MP-IL35	ADC	G3	1	0	0	Female	51
30	35-MP-IL35	ADC	G3	1b	0	0	Female	72
31	P1	SCC	G3	2	0	0	Female	66
32	P11	SCC	G3	2	0	0	Female	68
33	P15	SCC	G2	1b	0	0	Male	67
34	P18	SCC	G3	2a	0	0	Male	70
35	P19	SCC	G2	4	1	0	Male	48
36	P24	SCC	G2	2a	1	0	Male	61
37	P25	SCC	G3	2b	0	0	Male	72
38	P29	SCC	G2	2a	0	0	Female	69
39	P35	SCC	G2	1a	0	0	Male	45
40	1-MP-IL35	SCC	G3	1b	0	0	Male	80
41	2-MP-IL35	SCC	G3	1a	0	0	Male	57
42	4-MP-IL35	SCC	G3	1b	1	0	Female	53
43	5-MP-IL35	SCC	G2	3	0	0	Female	67
44	8-MP-IL35	SCC	G3	3	0	0	Male	66
45	13-MP-IL35	SCC	G3	1b	0	0	Male	69
46	14-MP-IL35	SCC	G2	1a	0	0	Female	58
47	21-MP-IL35	SCC	G1	1b	0	0	Male	41
48	29-MP-IL35	SCC	G3	1b	0	0	Male	74
49	30-MP-IL35	SCC	G3	1a	0	0	Female	70
50	36-MP-IL35	SCC	G3	2a	1	0	Male	74

T-extent of primary tumor: 0: No evidence of primary tumor; 1a: Tumor 2 cm or less in greatest dimension; 1b: Tumor more than 2 cm but not more than 3 cm in greatest dimension; 2a: Tumor more than 3 cm but not more than 5 cm in greatest dimension; 2b: Tumor more than 5 cm but not more than 7 cm in greatest dimension; 3: Tumor more than 7 cm; 4: Tumor of any size that invades the mediastinum, heart, great vessels, trachea, recurrent laryngeal nerve, esophagus, vertebral body, carina, or with separate tumor nodules in a different ipsilateral lobe.
N-regional lymph node metastasis: 0: No regional lymph node metastasis; 1: Metastasis in ipsilateral peribronchial and/or ipsilateral hilar lymph nodes and intrapulmonary nodes, including involvement by direct extension; 2: Metastasis in ipsilateral mediastinal and/or subcarinal lymph node(s).
M-peripheral metastasis: 0: No distant metastasis; 1: Distant metastasis.
Histopathological grading: G1: well differentiated; G2: moderately differentiated; G3: Poorly differentiated.
No information available.

up-regulated activated STAT3 in adenocarcinoma tumour cells as well as with increased levels of IL-6R in Th17 cells in adenocarcinoma as compared to the tumoural region of the squamous carcinoma. Thus, further supporting the possibility to use anti-Th17 immunostrategies to defeat lung adenocarcinoma as well as the presence of an auto-activation of STAT3 in the adenocarcinoma cells.

Loss of correlation between *BATF* and *STAT3* mRNA in the tumoural region of NSCLC. To start to investigate the correlation between *STAT3* mRNA expression and the pathway activated by IL-6 via IL-6R, we analysed the correlation between *BATF* and *STAT3* mRNA in the tumoural and control regions of adenocarcinoma and squamous carcinoma (Fig. 5). Here we found a positive correlation between *BATF* and *STAT3* mRNA in the control region of both adeno (Fig. 5a) and squamous (Fig. 5c) cell carcinoma. However, this positive correlation was lost in the tumoural region of both but especially in the tumoural region of adenocarcinoma (Fig. 5b, d). Taken together, these data suggest an IL-6R/BATF/STAT3 correlation in tumour free lung tissue. By

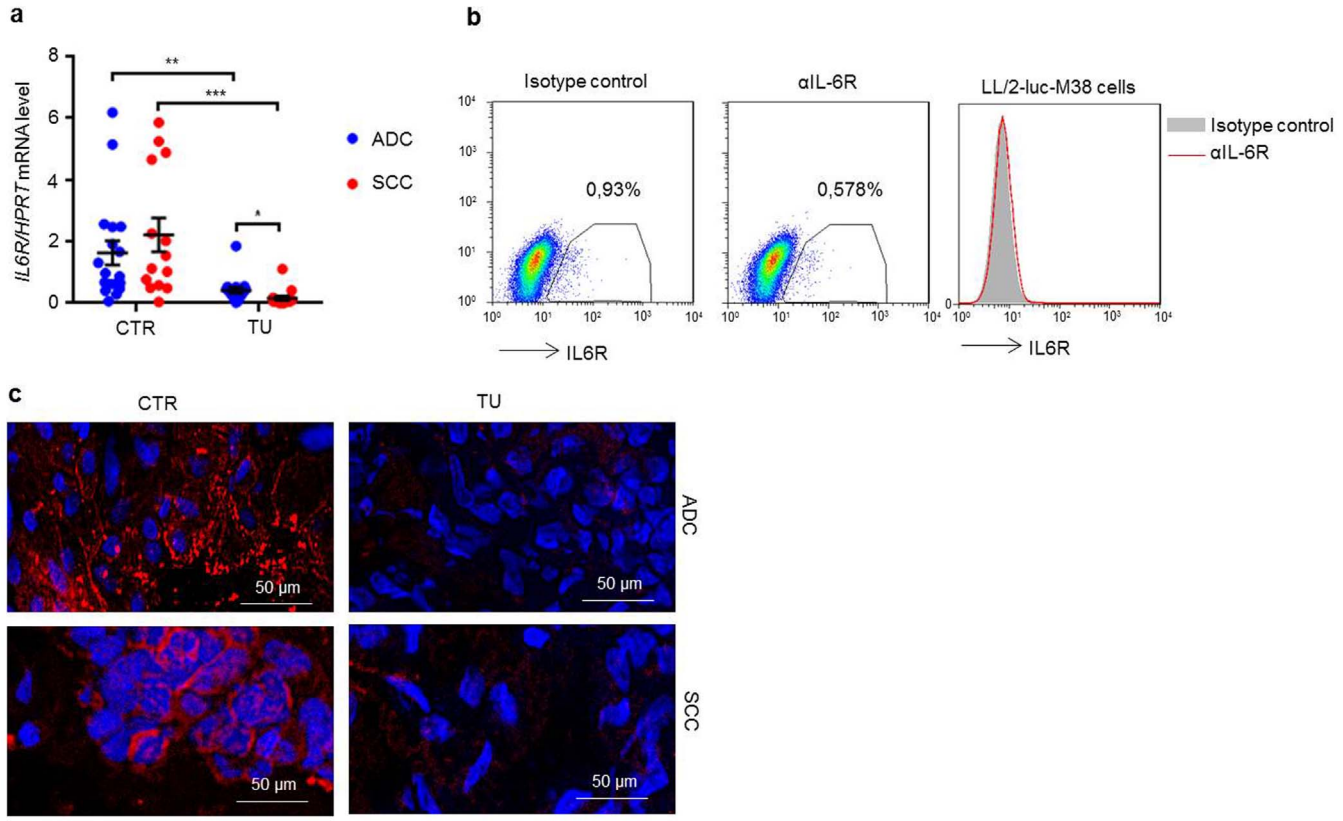

Figure 1 | Decreased *IL-6R* mRNA expression in the tumoural region of NSCLC. (a)- Quantitative Real-time PCR analysis of *IL-6R* mRNA expression in the tumoural and control lung area of patients with ADC (adenocarcinoma) and SCC (squamous cell carcinoma) (N ($ADC_{control}$)=18; N ($ADC_{tumoural}$)=17; N ($SCC_{control}$)=14; N ($SCC_{tumoural}$)=15). Data are shown as mean values ± s.e.m. using student's *t*-test **P*,0.05; ***P*,0.01; ****P*,0.001. (b) Flow cytometry staining of murine LL/2-luc-M38 tumour cells with an antibody against IL-6R and an isotype control antibody. (c)- Analysis of IL-6Rα protein expression by Immunohistochemistry (IHC) in the control and tumoural lung region of ADC as well as SCC.

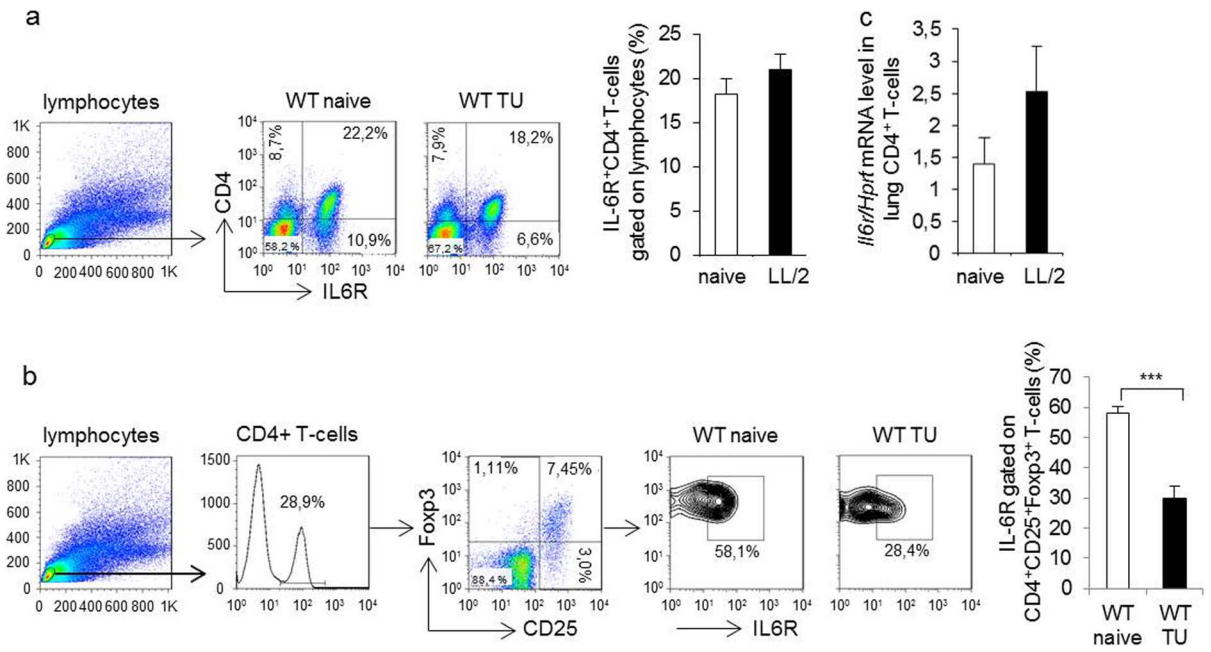

Figure 2 | Decreased expression of IL-6R on lung infiltrating CD4+CD25+Foxp-3+ T-cells in a murine model of lung cancer. (a),(b)- Flow cytometry analysis of IL-6R in the lungs of naïve as compared to LL/2-luc-M38 injected wild-type mice (N_{naive}=10, $N_{LL/2}$=11). a-Percentage of IL6R+CD4+ T-cells gated on lymphocytes. b- Percentage of IL-6R+cells gated on CD4+CD25+Foxp-3+ T-cells. Dot plots depict the gating strategy. Bar charts show the mean percentage of gated cells. Data are shown as mean values +/− s.e.m. using student's *t*-test ****P,0.001*.

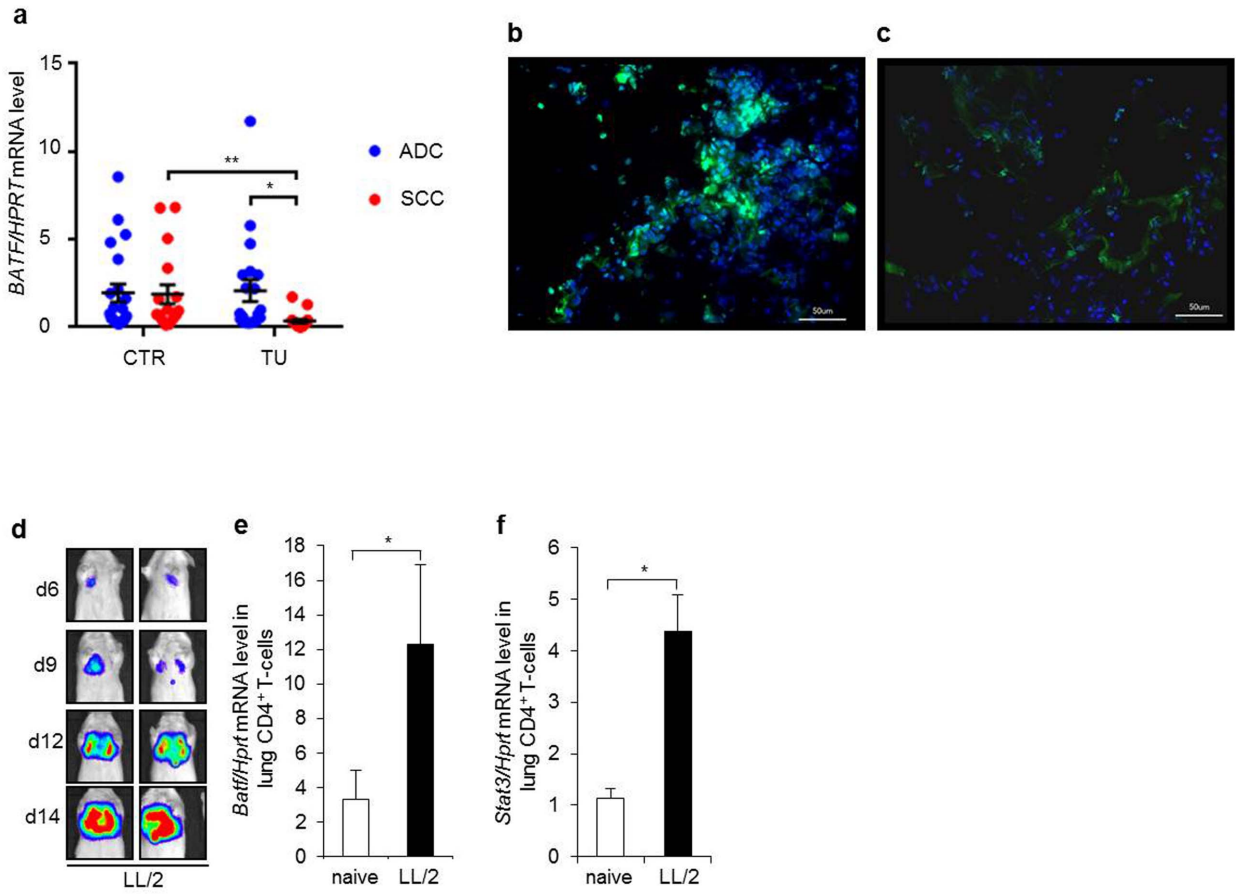

Figure 3 | Decreased *BATF* mRNA expression in the tumoural region of Squamous cell carcinoma. (a)- Quantitative Real-time PCR analysis of *BATF* (Basic leucine zipper transcription factor, ATF-like) mRNA expression in the tumoural and control lung area of patients with ADC (adenocarcinoma) and SCC (squamous cell carcinoma) (N ($ADC_{control}$)=21; N ($ADC_{tumoural}$)=20; N ($SCC_{control}$)=17; N ($SCC_{tumoural}$)=17). Data are shown as mean values ± s.e.m. using student's *t*-test **P*,0.05; ***P*,0.01. (b),(c)- Analysis of BATF protein expression by Immunohistochemistry (IHC) in the tumoural region of ADC (b) as compared to the tumoural region of SCC (c). d- Luciferase measurement of 2 representative mice injected with LL/2-luc-M38 cells. e,f- Quantitative Real-time PCR analysis of *Batf* and *Stat3* mRNA expression in CD4+ T-cells, isolated from the lungs of naïve as compared to tumour bearing wild-type mice and stimulated with anti-CD3 and anti-CD28 antibody. Data are shown as mean values ± s.e.m. using student's *t*-test **P*,0.05 (N= per group).

contrast in the tumour region auto-activation mechanisms of STAT3 might be BATF independent.

Increased *RORC* expression in the tumoural lung region of patients with adenocarcinoma as compared to those carrying lung squamous carcinoma. We next investigated whether the increase of *BATF* in ADC samples compared to SSC samples was accompanied by an increase of other Th17 specific transcription factors in the tumoural region. We found that *RORC,* a key Th17 transcription factor, was significantly up-regulated, like *BATF,* in the tumoural region of adenocarcinoma as compared to the tumoural region of the squamous carcinoma (Fig. 6). In addition, *RORC* like *BATF* was found significantly up-regulated in the control region as compared to the tumoural region of the squamous carcinoma. By contrast, a high and homogeneous distribution of *RORC* was found in the control and tumoural region of adenocarcinoma patients. In summary, RORγT is up-regulated in the tumoural region of adenocarcinoma compared to squamous cell carcinoma consistent with BATF and STAT3 up-regulation in this tumour.

Anti-IL-6R antibody treatment reduced Th17 and induced T regulatory cells. Since we found *Batf* mRNA increased in lung CD4+ T cells isolated from lung adenocarcinoma bearing mice, we then reasoned to block IL-6R signaling to see if the Th17 pathway would be down-regulated in a setting of lung adenocarcinoma. We therefore induced Lewis Lung adenocarcinoma growth in the lungs of mice and treated them intranasally with antibodies against the IL-6R (Fig. 7a). In the lungs of anti-IL-6R antibody treated mice we observed an increased number of CD4+CD25+Foxp3+ T regulatory lymphocytes compared to mice treated with IgG control antibodies (Fig. 7b), consistent with an inhibitory role of IL-6 for FOXP-3+ CD4+ T regulatory cell development. In affimetrix RNA gene arrays on CD4+ T cells isolated from the lungs of anti-IL-6R antibody treated mice, we observed a significant up-regulation of a series of immunosuppressive cytokines, such as *Il10*, *Il6* and *Il21* and of other genes known to be associated with regulatory cells like *Folr4*, *Ctla4*, *Icos*, *Il2ra* and *Lag3* (Fig. 7 c, d). By contrast, we detected a reduction of IL-17a expression. (Fig. 7e). Intranasal anti IL-6R antibody treatment significantly reduced also *Rorc* mRNA expression, encoding RORγT, a Th17 specific transcription factor in tumor-infiltrating lung CD4+ T cells both, by real time PCR and by RNA gene array on sorted lung CD4+ T cells, compared to IgG treatment (Fig. 7d–f). *Batf* did not show up either in the gene array analysis nor was found up-regulated by anti-IL-6R antibody treatment after real time PCR analysis (Fig. 7g). Taking together, these array data demonstrate an inhibitory function of IL-6 on T regulatory cell genes while favouring Th17 differentiation in a setting of adenocarcinoma. These data are consistent with our data on human samples.

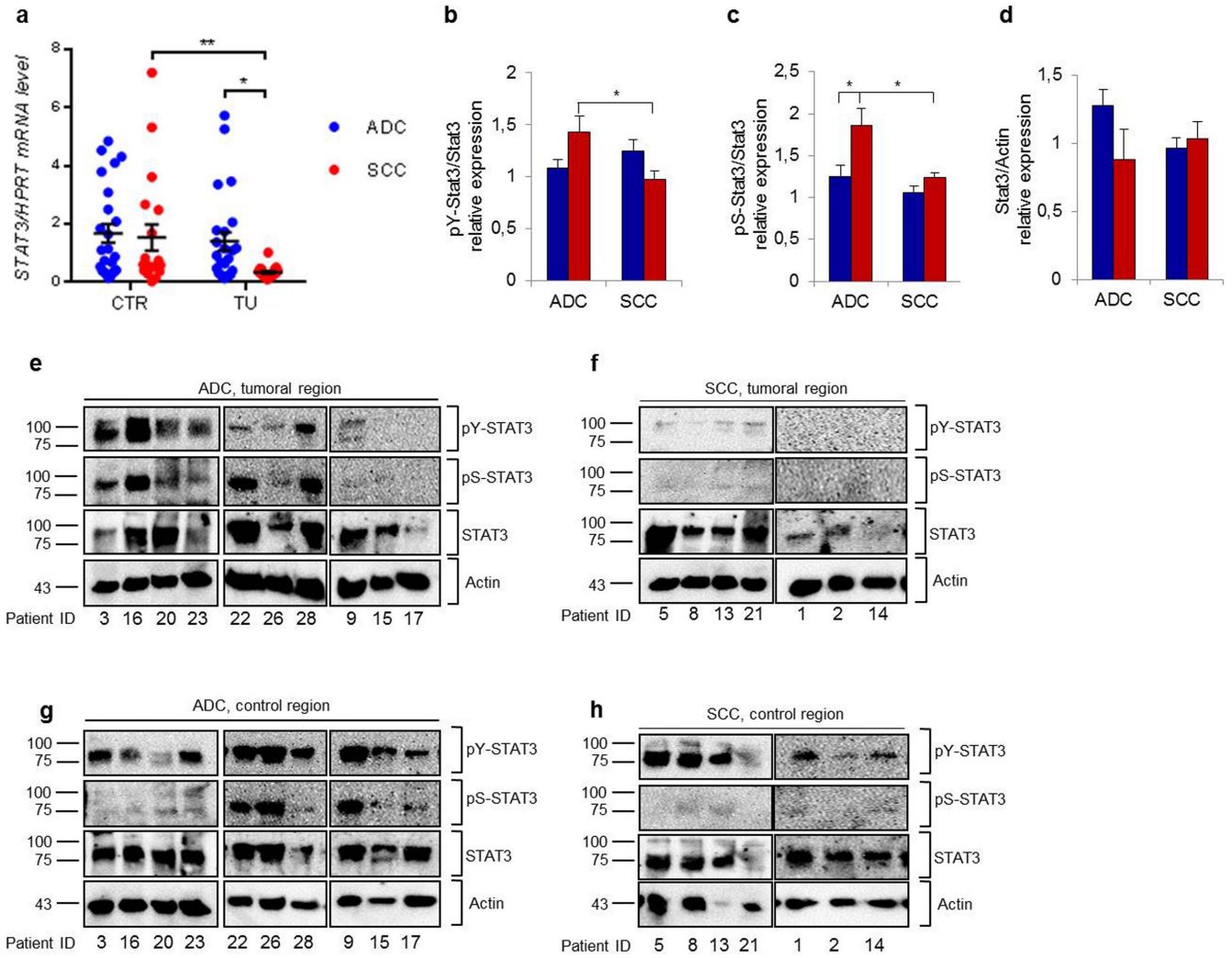

Figure 4 | Increased pSTAT3 activation in the tumoural region of the lung with adenocarcinoma. (a)- Quantitative Real-time PCR analysis of *STAT3* mRNA expression in the tumoural and control lung area of patients with ADC and SCC (N ($ADC_{control}$)=24; N ($ADC_{tumoural}$)=24; N ($SCC_{control}$)=19; N ($SCC_{tumoural}$)=19). Data are shown as mean values ± s.e.m. using student's *t*-test **P*,0.05; ***P*,0.01. (b)-(d)- Western blot analysis and quantification of protein levels of pY-Stat3 relative to Stat3 (b), pS-Stat3 relative to Stat3 (c) and Stat3 relative to Actin (d) in the control and tumoural lung area of patients with ADC as well as SCC (pY-Stat3: N (ADC)=7, N (SCC)=7; pS-Stat3:N (ADC)=7, N (SCC)=7; Stat3: N (ADC)=7, N (SCC)=7). Data are shown as mean values +/- s.e.m. using student's *t*-test **P*,0.05. e-h-Representative western blot for pY-Stat3, pS-Stat3, Stat3 and Actin in the control and tumoural lung area of patients with ADC as well as SCC.

Discussion

Here we found increased expression of *IL6R*, *RORC* and *BATF*, a Th17 lineage specific transcription factors in the tumoural region of lung tissue from patients with lung adenocarcinoma as compared to the tumoural region of lung tissue derived from patients with lung squamous cell carcinoma. Similarly, in the tumoural region of adenocarcinoma *STAT3*, a transcription factor downstream of IL-6R, was found to be increased and was activated via phosphorylation and autoposphorylation. By contrast, in the tumoural region of squamous carcinoma STAT3 was found inactivated and not phosphorylated indicating the lack of activation of this pathway in lung squamous cell carcinoma. This is a big difference and needs further attention in the design of new therapies against different kinds of non-small-cell lung cancer (NSCLC). In fact, squamous cell carcinomas usually develop in smokers, whereas lung adenocarcinoma is typical for non-smokers and thus more linked to genetic mutations.

To start to understand the distribution of IL-6R and its downstream signaling in lung tumour, we first analysed IL-6R expression in an adenocarcinoma cell line used to induce tumour. We could not find IL-6R expression here, consistent with the findings in humans showing increased *IL-6R* staining in the tumour free control regions of the lung in patients with NSCLC. Moreover, we described in this study down-regulation of IL-6R on the surface of CD4+CD25+FOXP-3+ T regulatory cells infiltrating the lung in experimental adenocarcinoma, indicating a new mechanism by which the adenocarcinoma tumour cells down-regulate IL-6R in T regulatory cells thus allowing local immunosuppression. BATF has been shown to be induced by STAT3 in mouse myeloid leukemic cells. Dominant negative form of STAT3 resulted in lower expression of BATF[11,12]. Thus, the increased auto-phosporylation of STAT3 in the tumoural region of adenocarcinoma might be part of a mutational linkage responsible for the up-regulation of BATF in this region both in tumour and in T cells surrounding the tumour. The exact cellular distribution of STAT3/BATF expression in the microenvironment and in the tumour cell itself needs further studies. However, we found here a positive correlation between *BATF* and *STAT3* in the control region and the loss of this correlation in the tumoural region. This indicates that in the tumoural region STAT3 expression is not dependent on BATF and *vice versa*. $Batf^{-/-}$ mice were shown to have normally differentiated Th1 and Th2 cells, but lacked

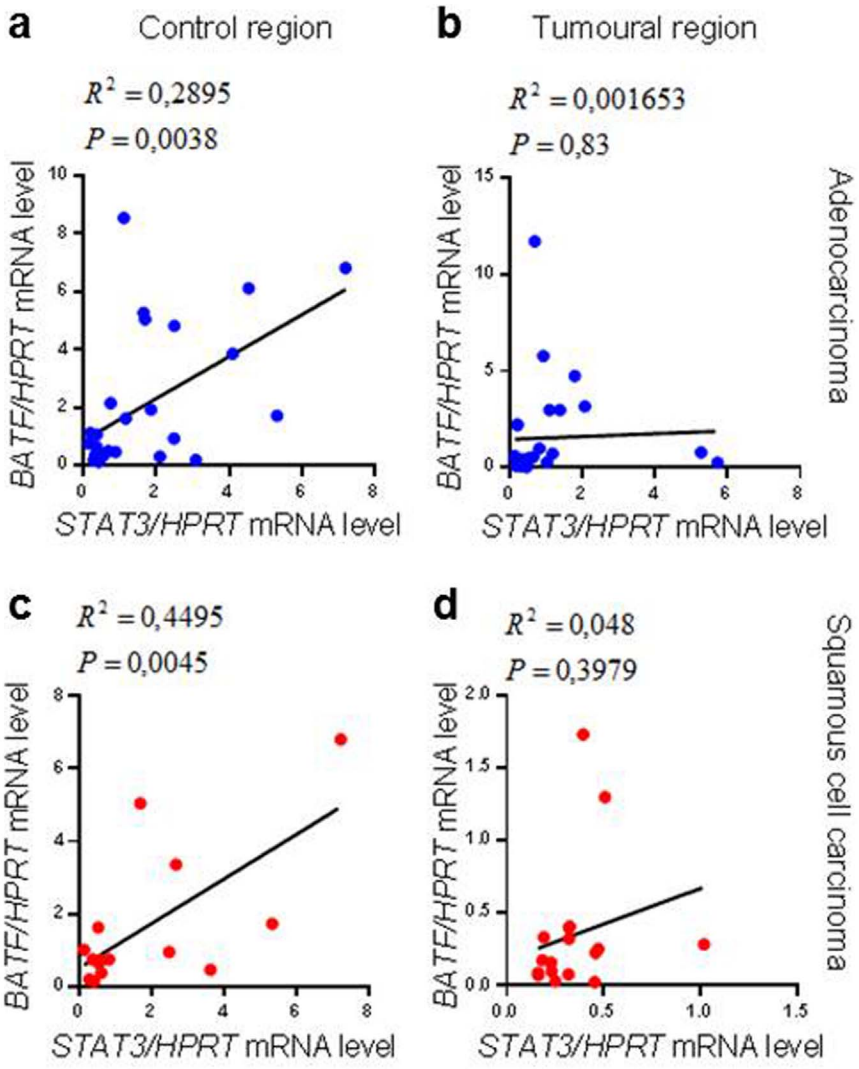

Figure 5 | *STAT3* mRNA level positively correlates with *BATF* mRNA expression in the control lung area of NSCLC. Correlation between *BATF* and *STAT3* mRNA expression in the control (a) and tumoural (b) lung area of patients with ADC as well as in the control (c) and tumoural (d) lung region of patients with SCC (N ($ADC_{control}$)=16; N ($ADC_{tumoural}$)=16; N ($SCC_{control}$)=17; N ($SCC_{tumoural}$)=17).

differentiated Th17 cells. When stimulated towards a Th17 lineage *in vitro*, $Batf^{-/-}$ T cells produced normal levels of IL-2, IFN-γ, and IL-10, but significantly reduced levels of IL-17. STAT3 and BATF have been described to bind to the IL-17A promoter, thus reinforcing the role of RORγT in this pathway[9,10,15]

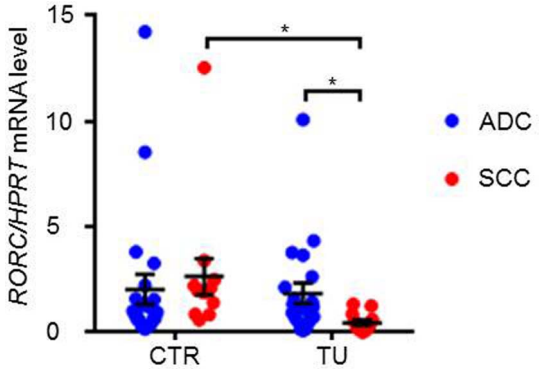

Figure 6 | *RORC* is reduced in the tumoural regions of SCC. Quantitaive Real-time PCR analysis of *RORC* mRNA expression in the tumoural and control lung area of patients with ADC and SCC (N ($ADC_{control}$)=22; N ($ADC_{tumoural}$)=21; N ($SCC_{control}$)=13; N ($SCC_{tumoural}$)=13). Data are shown as mean values ± s.e.m. using student's *t*-test *P,0.05.

In a murine model of adenocarcinoma we could demonstrate by using affimetix array that intranasal delivery of anti-IL-6R antibody but not IgG induced T regulatory immunosuppressive genes, such as *Il2ra*, *Ctla4*, *Icos*, *Folr4*, *Lag3*, *Il10*, *Il21* and *Foxp3*. Thus, IL-6 pathway inhibits T-regulatory cells and induces RORγT in lung tumour. Downstream of IL-6R cytokine receptor STAT3 is increased and phosphorylated in the tumoral region derived from adenocarcinoma bearing tissues[13]. Interestingly, none of the tumoural regions from patients with squamous carcinoma had activated pSTAT3, as shown by western blot analysis. This is consistent with the reduced *IL6R*, *BATF*, *RORC* expression in the squamous cell lung carcinoma.

Autophosphorylation of pSTAT3 favours mutations in this tumour. RORγT is also activated by pSTAT3. BATF, downstream of pSTAT3 favours IL-10 and IL-17A with RORγT. This IL-6R-BATF-STAT3-RORγT- axis seems an independently activated pathway in lung adenocarcinoma and not in squamous carcinoma. These findings have implication for the differential treatment of different histological types of lung tumour.

STAT3 is constitutively activated in different lung tumour cell lines and has been described to induce Th17 transcription factors

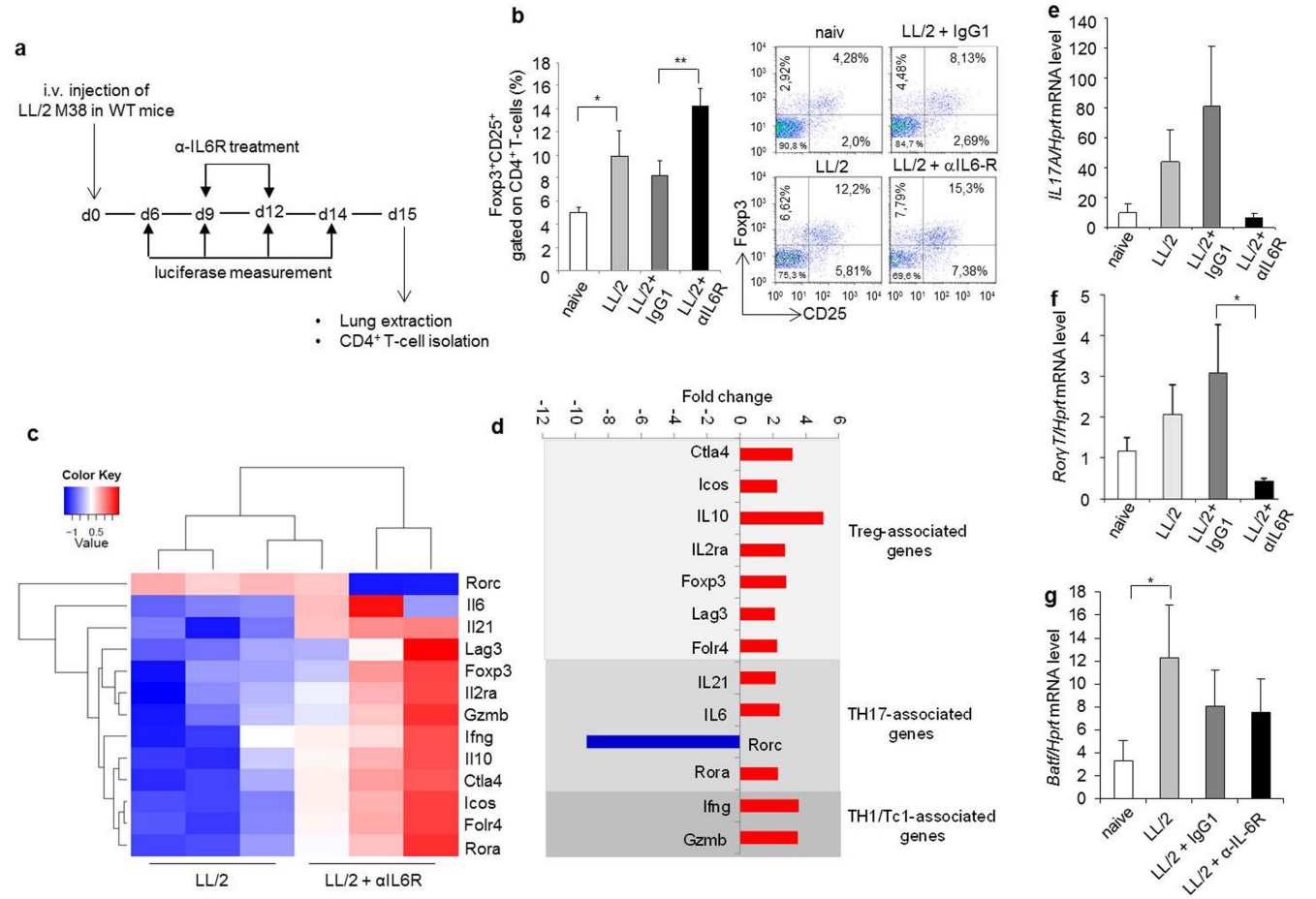

Figure 7 | Anti IL-6R antibody treatment did not ameliorate lung adenocarcinoma. (a)- Experimental design is shown. (b)- Flow cytometry analysis of Foxp-3+CD25+ cells gated on CD4+ lung T-cells from naïve or tumour bearing wild-type mice injected with LL/2-luc-M38 cells and treated with anti-IL6R antibody or IgG1 isotype control as compared to untreated mice. Data are shown as mean percentage ± s.e.m. using student's *t*-test **P*,0.05; ***P*,0.01 (N = 10–11 per group). (c),(d)-Gene array analysis of RNA, isolated from $CD4^+$ lung T-cells of tumour bearing wild-type mice treated with anti-IL6R antibody or untreated. The fold-change of the mRNA expression of significantly altered genes is shown as a heatmap (c) and as a bar chart (d) (N = 3 per group). (e),(f),(g)- Quantitative Real-time PCR analysis of *Il17* (e), *Rorc* (f) and *Batf* (g) mRNA expression in CD4+ T-cells, cultured with anti-CD3 and anti-CD28 antibody. $CD4^+$ T-cells were isolated from the lungs of naïve or tumour bearing wild-type mice injected with LL/2-luc-M38 cells and treated with anti-IL6R antibody or IgG1 isotype control compared to untreated mice. Data are shown as mean values ± s.e.m. Sudent's t-test was used. * P,0.05 (N = 10–11 per group).

such as BATF and RORγT. However, IL-6 also inhibits the immunosuppressive marker FOXP-3 explaining why anti IL-6R antibody treatment would be not effective in adenocarcinoma. Thus, it is possible that a better target than IL-6R would be targeting the BATF activity in lung adenocarcinoma, because it could result in a blockade of the immune evasion activated by the adenocarcinoma because this transcription factor induces the immunosuppressive cytokine IL-10 in addition to IL-17A[16]. Moreover, we have described recently that BATF deficient mice have reduced STAT5 and FOXP-3+ T regulatory cells[15]. Since STAT5 deficient mice have less FOXP-3 regulatory T cells[17], targeting BATF would have many advantages over blockade of IL6R because it would inhibit IL-10, STAT5 and IL-17A and probably it would reduce immunosuppression in lung tumours like adenocarcinoma via IL-6. In summary, this work advances our understandings on the IL-6R activated pathway in T cells and in tumour cell adenocarcinoma. Moreover, it shows that in human squamous cell carcinoma and its microenvironment this pathway is not activated. It further highlights a possible negative effect of targeting IL-6R in adenocarcinoma tumour because it would induce immunosuppression. We further identified BATF as a possible better target for adenocarcinoma therapy.

Methods

All the methods described in this manuscript were carried out in accordance with the approved guidelines. Moreover, all the human studies and their experimental protocols were approved by the local ethics review board of the University of Erlangen (Re-No: 56_12B;) and registered at DRKS-ID: DRKS00005376 available online.

The experiment protocols performed in this study in mice were approved by the "Regierung Mittelfranken" in the "Asthma und Lungentumormodelle" file number :Az. 54.2532.1-2/10.

Human subjects and study population. The study was performed at the University of Erlangen in Germany in agreement with the local ethics review board of the University of Erlangen. Patients' confidentiality was maintained and informed consent was obtained from each patient. The histological types of lung cancer were classified according to the histological classification of the World Health Organization (WHO), formulated in 2004. The staging of lung cancer was based on the Cancer TNM Staging Manual, formulated by the International Association for the Study of Lung Cancer (IASLC) in 2010. As shown in Table I, this study was done by analyzing samples stored frozen immediately after thoracic surgery was performed and transported to the adjacent Pathology Department at the University of Erlangen (CCC-Bank). From the pathology, the remaining material was immediately sectioned to divide the tumoural area from the peritumoural (2 cm surrounding the tumoural region) and the control region taken at least 5 cm far from the tumoural region (Fig. S1). Immediately after, the lung pieces were transported on ice to the department of Molecular Pneumology at the University of Erlangen and there stored frozen immediately. This study is registered at the "Deutsches Register Klinischer Studien". Registration number DRK S00005376.

Quantitative Real-Time PCR (qPCR) human. Total RNA was extracted from frozen tissue samples using peqGold RNA Pure (peqlab, Erlangen, Germany) according to manufacturer's instructions. 1 µg of the resulting RNA was reverse-transcribed into cDNA via the RevertAid™ First Strand cDNA Synthesis Kit (Fermentas, St. Leon-Rot, Germany) according to manufacturer's protocol. Each qPCR reaction mix contained 15 ng of cDNA, 300 nM transcript-specific forward and reverse primer and 2x SsoFast™ EvaGreen® Supermix (BIO-RAD, Munich, Germany) in a total volume of 20 µl. QPCR primers were purchased from Eurofins-MWG-Operon, Ebersberg, Germany. The primer sequences are given for *HPRT* (fw: 5′-TGA CAC TGG CAA AAC AAT GCA-3′; rev: 5′- GGT CCT TTT CAC CAG CAA GCT-3), *BATF* (fw: 5′-AGC GAA GAC CTG GAG AAA CA-3′; rev: 5′- TTC AGC ACC GAC GTG AAG TA-3′), *IL6R* (fw: 5′- GAC AAT GCC ACT GTT CAC TG-3′; rev: 5′-GCT AAC TGG CAG GAG AAC TT-3′), *RORC* (fw: 5′- TGA GAA GGA CAG GGA GCC AA-3′; rev: 5′-CCA CAG ATT TTG CAA GGG ATC A-3′), *STAT3* (fw: 5′-TTT GTC AGC GAT GGA GTA CG-3′; rev: 5′- GCT GCA ACT CCT CCA GTT TC-3′). Reactions were performed for 50 cycles with an initial activation for 2 minutes at 98°C, denaturation for 5 min at 95°C and hybridization and elongation for 10 min at 60°C. QPCR reactions were performed using the CFX-96 Real-Time PCR Detection System (BIO-RAD, Munich, Germany), and analysed via the CFX Manager Software. The relative expression level of specific transcripts was calculated with respect to the internal standard, HPRT. Expression levels were normalized to Control lung tissues using ΔΔCT calculation.

BATF Immunohistochemistry. Immunohistochemistry for BATF was performed in collaboration with the Institute of Anatomy at the University of Erlangen on 6 µm thick cryosections from lung tissue taken from the tumoural or control lung area (at least 5 cm far away from the tumour region) of patients with adenocarcinoma and squamous cell carcinoma. The sections were stored frozen until staining was performed. The sections were fixed for 5 minutes with 4% paraformaldehyde in PBS at room temperature followed by three washes 10 minutes each in PBS. To avoid not-specific staining lung tissue sections were incubated in Blotto (InVitrogen) for 1 hour. The primary antibody, anti-human BATF made in rabbit (D7C5, Cell Signaling Technology) was then applied (working dilution1 : 200 in PBS) to the tissue sections overnight at 4°C in a humid incubation chamber.

Next day, sections were washed three times in PBS. Slides were then incubated for additional 30 minutes in PBS under shaking conditions. At this point the secondary antibody goat anti Rabbit Alexa 488 (Invitrogen) (1 : 200 in PBS) was applied in the dark for 1 hour. The residual secondary antibody was washed out with three washes with PBS.

The cell nuclei were then stained with DAPI (4′,6-diamidine-2-phenylindol-dihydrochloride; Boehringer, Mannheim) by embedding the sections in DAPI-glycerol solution (PBS-glycerol 1 : 1, adding 10 µl of 2 mg/ml DAPI stock solution). The slides were then examined with a Keyence Biozero BZ9000 microscope (Keyence Deutschland, Neu-Isenburg, Germany).

IL-6R alpha Immunohistochemistry. The Immunohistochemistry (IHC) for IL-6R was performed as described above for BATF- IHC with the following modifications. The primary antibody, mouse monoclonal anti-human IL-6R-gp80 (Invitrogen) was applied to the tissue sections overnight at 4°C in a humid incubation chamber at the working dilution 1 : 50 in PBS.

Next day, sections were washed three times in PBS and then incubated for additional 30 minutes in PBS under shaking conditions. At this point the secondary antibody Rhodamin conjugated anti mouse made in goat (Invitrogen) (1 : 700 in PBS) was applied in the dark for 1 hour. The residual secondary antibody was washed out with three washes with PBS.

The cell nuclei were then stained with DAPI (4′,6-diamidine-2-phenylindol-dihydrochloride; Boehringer, Mannheim) by embedding the sections in DAPI-glycerol solution (PBS-glycerol 1 : 1, adding 10 µl of 2 mg/ml DAPI stock solution). The slides were then examined with a Keyence Biozero BZ9000 microscope (Keyence Deutschland, Neu-Isenburg, Germany).

Protein isolation and western blot analyses. Lung tissue samples were lysed using protein lysis buffer (1% NP40, 20 mM pH8 Tris HCL, 137 mM NaCl, 5% Glycerin, 2 mM EDTA, Complete Mini EDTA free (Roche Diagnostics, Mannheim, Germany)), homogenized and sonicated in an ultrasonic bath for 2 min., followed by 15 min. of incubation on ice and centrifugation (30 min., 4°C, 12000 rpm). The supernatant containing the proteins was collected and protein concentration was determined via Bradford assay. Each western blot sample contained 30–50 µg protein and 5 µl sample buffer (4x Roti-Load, Roth, Karlsruhe, Germany) in a total volume of 20 µl. Samples were heated at 95°C for 5 min. and subsequently cooled on ice prior to loading onto 10% polyacrylamide gel. Polyacrylamide gel electrophoresis was performed at 80 V for 1,5 h. Proteins were then transferred to a nitrocellulose membrane (PAGEr Ex Gels, Lonza, Rockland, USA) at 200 mA for 45 min. The membrane was washed with 0,05% Tween20 in PBS for 5 min. After 1 h of incubation in blocking buffer (5% milk powder, 0,1% Tween20 in PBS) at room temperature, the primary antibody was applied and incubated over night at 4°C. The next day the membrane was washed 3 times in PBST (0,1%Tween20) for 5 min each. The membrane was incubated with the HRP-conjugated secondary antibody, soaked in blocking buffer, for 1 h at room temperature. After that, the membrane was washed twice with PBST (0,1% Tween20) and once with PBS, for 5 min each. For detection of the proteins the Western Bright Quantum Western Blotting detection kit (Biozym Scientific, Oldendorf, Germany) was used according to manufacturer's protocol. For the visualization of the western blot results the Fluor Chem FC2 (Biozym Scientific, Oldendorf, Germany) detection system was used. The following antibodies were used pStat3 (Y705) (Cell Signaling Technology, Danvers, USA), pStat3 (S727) (Cell Signaling Technology, Danvers, Massachusetts, USA), Stat3 (Santa Cruz Biotechnology, Dallas, Texas, USA), Actin (Santa Cruz Biotechnology, Dallas, Texas, USA).

Cell Lines. The LL/2-luc-M38 cell line (Bioware cell line, Caliper LifeScience, Waltham, Massachussets, USA) was cultured in DMEM-medium, supplemented with 10% of fetal calf serum (FCS) (Biofluids) and 1% of the antibiotics penicillin and streptavidin (Pen/Strep) (Gibco, Invitrogen) at 37°C and 5% of CO_2.

Mice. BALB/cJ wild-type mice were maintained under specific pathogen-free conditions at the animal facility adjacent to our laboratories. Experiments were performed in accordance to protocols approved by the local Ethical committee.

Murine model for lung adenocarcinoma and antibody treatment. The Lewis lung carcinoma model was induced via injection of 5×10^5 LL/2-luc-M38 cells (Bioware cell line, Caliper LifeScience, Waltham, Massachussets, USA) resuspended in 200 µl of DMEM media (Gibco, Invitrogen, Darmstadt, Germany) without supplements into the tail vein of 6–8 week old mice. Prior to injection, LL/2-luc-M38 cells were cultured with DMEM media, containing 10% fetal calf serum (FCS; Biofluids) and 1% Penicillin/Streptomycin antibiotics (Gibco, Invitrogen, Darmstadt, Germany) at 37°C and 5% of CO_2. At day 9 and 12 after tumour induction mice were treated with 90 µg of αIL6R antibody (Chugai Pharmaceuticals, Japan) or IgG1 Isotype control (R&D Systems, Minneapolis, USA), resolved in 45 µl of PBS, intranasally (i.n.). Mice were sacrificed at day 15 after tumour cell injection. Lungs were removed and analysed as described below.

Tumour load analysis. Tumour load was analysed *in vivo* at day 6, 9 and 12 and 14 after injection of LL/2-luc-M38 cells using the Ivis Imaging System (Bioware cell line, Caliper LifeScience, Waltham, Massachussets, USA). For that purpose mice were injected with 150 µl of Luciferin solution (15 mg/ml) intraperitoneally (i.p.) (Promega, Madison, Wisconsin, USA). After 10 min of incubation luminescence, emitted by the LL/2-luc-M38 cells in the lungs of the mice, was measured. The analysis was done in a logarithmic scale mode. For quantification of the tumour load the total flux (photons per second) was determined.

Flow cytometry staining. Flow cytometry analyses were performed with 1×10^6 total cells per sample and staining. The cells were washed with PBS, followed by incubation (30 min., 4°C, dark) with the respective mix of antibodies against surface proteins, solved in PBS (ad 80 µl). After an additional washing step the cells were fixed and permeabilized with Fixation/Permeablilization solutions according to manufacturer's protocol (eBioscience) and incubated (30 min, 4°C, dark) with antibodies against intracellular proteins, solved in Permeabilization buffer (eBiosience) (ad 80 µl). After a final washing step with Permeabilization buffer (eBiosience) the cells were resuspended in PBS+ EDTA (Lonza). For FACS analyses of surface markers alone, the cells were washed with PBS and resuspended in PBS+ EDTA (Lonza) after incubation with the surface antibodies. No fixation and permeabilization was performed in that case. The subsequent flow cytometry measurements were performed via FACS Calibur and analyzed using Cell Quest Pro version 4.02 (BD Biosciences, Heidelberg, Germany). The following antibodies were used during this study. Anti-mouse CD4 FITC (BD Bioscience, Heidelberg, Germany), Anti-mouse CD25 PerCP (BD Bioscience, Heidelberg, Germany), Anti-mouse IL6R (eBioscience, Frankfurt, Germany), Anti-human/mouse FOXP3 APC (Miltenyi Biotec, Bergisch-Gladbach, Germany).

CD4+ T-cell isolation. Single cell suspensions from murine lungs were prepared as previously described[18]. Isolation of $CD4^+$ T-cells from total lung cells was performed using anti-mouse CD4 Microbreads (Miltenyi Biotec, Bergisch-Gladbach, Germany) by positive selection according to manufacturer's protocol. CD4+ T-cells were cultured in RPMI medium, supplemented with 10% FCS and 1% Pen/Strep, at 37°C and 5% CO_2, in the presence of 5 µg/ml plate bound anti-mouse CD3 antibody (BD Biosciences) and 2 µg/ml soluble anti-mouse CD28 antibody (BD Biosciences).

Quantitative Real-Time PCR (qPCR) in mouse samples. Total RNA was extracted from lung derived CD4+ T-cells, using peqGold RNA Pure (peqlab, Erlangen, Germany) according to manufacturer's instructions. 1 µg of the resulting RNA was reverse-transcribed into cDNA via the RevertAid™ First Strand cDNA Synthesis Kit (Fermentas, St. Leon-Rot, Germany) according to manufacturer's protocol. Each qPCR reaction mix contained 15 ng of cDNA, 300 nM transcript-specific forward and reverse primer and 2x SsoFast™ EvaGreen® Supermix (BIO-RAD, Munich, Germany) in a total volume of 20 µl. QPCR primers were purchased from Eurofins-MWG-Operon, Ebersberg, Germany. The primer sequences are given for *Hprt* (fw: 5′-GCC CCA AAA TGG TTA AGG TT-3′; rev: 5′- TTG CGC TCA TCT TAG GCT TT-3′), *Batf* (fw: 5′-GTT CTG TTT CTC CAG GTC C-3′; rev: 5′- GAA GAA TCG CAT CGC TGC-3′), *Il17A* (fw: 5′- TCC AGA AGG CCC TCA GAC TA-3′; rev: 5′-ACA CCC ACC ACA TCT TCT C-3′), *Rorγt* (fw: 5′- GTG TGC TGT CCT GGG CTA CC-3′; rev: 5′- AGC CCT TGC ACC CCT CAC AG-3′), *Il6r* (fw: 5′-GCC CAA ACA CCA AGT CAA CT-3′; rev: 5′- TAT AGG AAA CAG CGG GTT GG-3′), Stat3 (fw: 5′- GCT TCC TGC AAG AGT CGA AT-3′; rev: 5′- ATT GGC TTC TCA AGA TAC CTG-3′). Reactions were performed for 50 cycles with an initial activation for

2 min at 98°C, denaturation for 5 min at 95°C and hybridization and elongation for 10 min at 60°C. QPCR reactions were performed using the CFX-96 Real-Time PCR Detection System (BIO-RAD, Munich, Germany), and analysed via the CFX Manager Software. The relative expression level of specific transcripts was calculated with respect to the internal standard, HPRT. Expression levels were normalized to Control lung tissues using ΔΔCT calculation.

Gene Array. In collaboration with the Institute of Human Genetics at the University of Erlangen (prof A. Ekici) a gene array was performed. Briefly, RNA was isolated from lung CD4+ T-cells of LL/2-luc-M38 injected wild-type mice that were either untreated, treated with anti-IL6R antibody or with IgG1 isotype control as described above. After quality control analysis of the isolated RNA, the GeneChip® Gene 1.0 ST Array (Affymetrix, Santa Clara, USA) was used for further analysis.

Statistical analysis. Differences were evaluated for significance ($P<0.05$) by the unpaired student's t-test using the GraphPad PRISM software. Data are given as mean values ± s.e.m.

1. Aberle, D. R. *et al.* Results of the two incidence screenings in the National Lung Screening Trial. *N Engl J Med* **369**, 920–931, doi:10.1056/NEJMoa1208962 (2013).
2. Maus, M. K. *et al.* KRAS mutations in non-small-cell lung cancer and colorectal cancer: Implications for EGFR-targeted therapies. *Lung cancer*, doi:10.1016/j.lungcan.2013.11.010 (2013).
3. Kang, H. J. *et al.* Comparison of clinical characteristics between patients with ALK-positive and EGFR-positive lung adenocarcinoma. *Respir Med*, doi:10.1016/j.rmed.2013.11.020 (2013).
4. Song, L., Rawal, B., Nemeth, J. A. & Haura, E. B. JAK1 activates STAT3 activity in non-small-cell lung cancer cells and IL-6 neutralizing antibodies can suppress JAK1-STAT3 signaling. *MCT* **10**, 481–494, doi:10.1158/1535-7163.MCT-10-0502 (2011).
5. Andreev, K., Graser, A., Maier, A., Mousset, S. & Finotto, S. Therapeutical measures to control airway tolerance in asthma and lung cancer. *Front Immunol* **3**, 216, doi:10.3389/fimmu.2012.00216 (2012).
6. Acosta-Rodriguez, E. V., Napolitani, G., Lanzavecchia, A. & Sallusto, F. Interleukins 1beta and 6 but not transforming growth factor-beta are essential for the differentiation of interleukin 17-producing human T helper cells. *Nat Immunol* **8**, 942–949, doi:10.1038/ni1496 (2007).
7. Senga, T. *et al.* Stat3-dependent induction of BATF in M1 mouse myeloid leukemia cells. *Oncogene* **21**, 8186–8191, doi:10.1038/sj.onc.1205918 (2002).
8. Liu, X., Lee, Y. S., Yu, C. R. & Egwuagu, C. E. Loss of STAT3 in CD4+ T cells prevents development of experimental autoimmune diseases. *J Immunol* **180**, 6070–6076 (2008).
9. Yang, X. O. *et al.* STAT3 regulates cytokine-mediated generation of inflammatory helper T cells. *J Biol Chem* **282**, 9358–9363, doi:10.1074/jbc.C600321200 (2007).
10. Hirahara, K. *et al.* Signal transduction pathways and transcriptional regulation in Th17 cell differentiation. *Cytokine Growth Factor Rev* **21**, 425–434, doi:10.1016/j.cytogfr.2010.10.006 (2010).
11. Liao, J., Humphrey, S. E., Poston, S. & Taparowsky, E. J. Batf promotes growth arrest and terminal differentiation of mouse myeloid leukemia cells. *MCR* **9**, 350–363, doi:10.1158/1541-7786.MCR-10-0375 (2011).
12. Yu, H., Pardoll, D. & Jove, R. STATs in cancer inflammation and immunity: a leading role for STAT3. *Nat Rev Cancer* **9**, 798–809, doi:10.1038/nrc2734 (2009).
13. Koch, S. *et al.* IL-6 activated integrated BATF/IRF4 functions in lymphocytes are T-bet-independent and reversed by subcutaneous immunotherapy. *SciRep* **3**, 1754, doi:10.1038/srep01754 (2013).
14. Doganci, A. *et al.* The IL-6R alpha chain controls lung CD4+CD25+ Treg development and function during allergic airway inflammation in vivo. *J Clin Invest* **115**, 313–325, doi:10.1172/JCI22433 (2005).
15. Ubel, C. *et al.* The activating protein 1 transcription factor basic leucine zipper transcription factor, ATF-like (BATF), regulates lymphocyte- and mast cell-driven immune responses in the setting of allergic asthma. *J Allergy Clin Immunol* **133**, 198–206 e191-199, doi:10.1016/j.jaci.2013.09.049 (2014).
16. Li, P. *et al.* BATF-JUN is critical for IRF4-mediated transcription in T cells. *Nature* **490**, 543–546, doi:10.1038/nature11530 (2012).
17. Burchill, M. A., Yang, J., Vang, K. B. & Farrar, M. A. Interleukin-2 receptor signaling in regulatory T cell development and homeostasis. *Immunol Lett* **114**, 1–8, doi:10.1016/j.imlet.2007.08.005 (2007).
18. Sauer, K. A., Scholtes, P., Karwot, R. & Finotto, S. Isolation of CD4+ T cells from murine lungs: a method to analyze ongoing immune responses in the lung. *Nat Protoc* **1**, 2870–2875, doi:10.1038/nprot.2006.435 (2006).

Acknowledgments

The authors thank Sonja Trump, Adriana Geige at the Molecular Pneumology department at the University of Erlangen for their technical support. The authors are also grateful to Prof. Arif Ekici and his team especially Dr. Fulvia Ferrazzi from the Institute of Human Genetic at the University of Erlangen, in Erlangen for performing and analysing with us the Gene Arrays. This work was supported by the IZKF grant A59 and by the Molecular Pneumology Department in Erlangen.

Author contributions

S.F. designed the experiments and L.B., K.A., N.B. performed the experiments presented in this study. K.A. analysed all the data in the paper. M.S., M.M. and S.R. helped with the experimental part of the study. D.I.T., T.R., H.S. and A.H. are responsible for the clinical part of this study. Martin Schicht and L.B. performed and analysed IHC for BATF and IL-6R. S.F. supervised the research, analysed the data and wrote the manuscript.

Additional information

The present work was performed in fulfilment of the requirements for obtaining the degree "Dr. med." of Ljubov Balabko at the Friedrich-Alexander-University Erlangen-Nürnberg (FAU), Erlangen.

Supplementary information accompanies this paper at http://www.nature.com/scientificreports

Competing financial interests: The authors declare no competing financial interests.

How to cite this article: Balabko, L. *et al.* Increased expression of the Th17-IL-6R/pSTAT3/BATF/Rorγ T-axis in the tumoural region of adenocarcinoma as compared to squamous cell carcinoma of the lung. *Sci. Rep.* **4**, 7396; DOI:10.1038/srep07396 (2014).